

# Energetic limitations and mass mortality of Bering Sea snow crab: Interacting effects of warming and density on collapse and recovery

Erin J. Fedewa<sup>1\*</sup>, Louise A. Copeman<sup>2</sup> and Michael A. Litzow<sup>1</sup>

<sup>1</sup>Alaska Fisheries Science Center, National Marine Fisheries Service, 301 Research Court, Kodiak, AK 99615, USA

<sup>2</sup>Alaska Fisheries Science Center, National Marine Fisheries Service, 2030 SE Marine Science Dr.,  
Newport, OR 97365, USA

\*Corresponding author: erin.fedewa@noaa.gov

## ORCHID IDs

Erin J. Fedewa: 0009-0009-4965-8886

Louise A. Copeman: 0000-0002-8851-7586

Michael A. Litzow: 0000-0003-1611-4881

18 **ABSTRACT**

19 Marine heatwaves can result in mass mortality events, but the mechanisms underlying population collapse  
20 and recovery dynamics are often poorly understood. Here, we employed a comparative analysis between  
21 collapsing and non-collapsing portions of the Bering Sea snow crab population to evaluate linkages  
22 between energetic condition and population abundance during and after a recent collapse. We show that  
23 abundance declines during the collapse were associated with dramatic declines in energetic condition, and  
24 the negative impact of high population density on energetic reserves was intensified by warming during a  
25 marine heatwave. Elevated energetic condition coincided with strong recruitment post-collapse,  
26 suggesting rapid initial population recovery in the eastern Bering Sea. However, we show that cold-water  
27 habitat ( $\leq 0^{\circ}\text{C}$ ) is critical for supporting high snow crab density in rebuilding towards a pre-collapse state.  
28 These results suggest that warming and loss of sea ice will exacerbate the risk of collapse in snow crab  
29 through energetic constraints on survival. Furthermore, we highlight the validation of an indirect  
30 energetic condition metric that will facilitate continued energetics monitoring and rapid integration into  
31 management.

32

33

34 *Key words: Bering Sea, Chionoecetes opilio, energetics, fatty acids, marine heatwave, population*  
35 *collapse*

36

37 **INTRODUCTION**

38 Climate change is rapidly increasing thermal risk for populations, and mass mortality events  
39 related to marine heatwaves are increasingly common, most notably for invertebrates (Fey et al. 2015).  
40 Discrete and prolonged periods of anomalously warm water that define marine heatwaves have increased  
41 in frequency, duration and spatial extent during the past decade in northern latitudes such as the Bering  
42 Sea (Hobday et al. 2016; Carvalho et al. 2021). Snow crab (*Chionoecetes opilio*),

43 in particular, are highly vulnerable to marine heatwaves, as they are highly stenothermic and rely on cold  
44 bottom waters associated with seasonally ice-covered habitats. Recent and rapid sea ice loss in  
45 the Bering Sea have exacerbated the loss of these cold-water habitats, and predictions of ice-free  
46 conditions in coming decades raise concern for ice-associated species (Wang and Overland 2012; Notz  
47 and Stroeve 2016; Overland and Wang 2025). During 2018-2019, a marine heatwave in the Bering Sea  
48 resulted in the lowest winter sea ice extent on record and extreme bottom water warming (Stabeno and  
49 Bell, 2019). The snow crab population in the eastern Bering Sea abruptly collapsed following the marine  
50 heatwave, declining from the highest-observed abundance in 2018 to the lowest-observed in 2021  
51 (Szuwalski et al. 2023). The highly valuable fishery for Bering Sea snow crab was subsequently closed  
52 for the first time in history during the 2022-2023 and 2023-2024 seasons.

53 Considered one of the largest mass mortality events of motile marine macrofauna in recent  
54 history, the snow crab collapse was attributed to the 2018-2019 marine heatwave and unprecedented sea  
55 ice loss (Szuwalski et al. 2023; Litzow et al. 2024). In particular, elevated snow crab mortality during the  
56 collapse was linked to high population density and a temperature-driven increase in metabolic demand,  
57 suggesting that starvation was the proximate cause for the collapse. However, these conclusions  
58 concerning the role of starvation were drawn, in part, from reductions in snow crab body weight-at-size  
59 (Szuwalski et al. 2023), despite evidence that morphological indices of condition are highly insensitive in  
60 detecting energy depletion and starvation-induced mortality in snow crab (Hardy et al. 2000; Lorentzen et  
61 al. 2020; Kruse 2023). Biochemical indices (e.g., lipid and fatty acid content) provide direct estimates of  
62 energetic condition (Copeman et al. 2018; Copeman et al. 2021) and, as such, are better suited to evaluate  
63 energetic constraints and bottom-up food limitation (Stevenson and Woods 2006). Energetic status can  
64 have a strong effect on starvation and mortality risk, and declines in population abundance are often  
65 closely linked to reduced energetic condition (Dutil and Lambert 2000). Likewise, energetic metrics  
66  
67 (Mullowney and Rose 2014; Receveur et al. 2022), while rebounding energetic condition can

68 reflect population recovery. Despite the potential for energetic condition indices to improve our  
69 understanding of population fluctuations and to provide early detection of impending mortality events,  
70 energetic condition is not routinely monitored in Bering Sea snow crab. This paucity of data is, in part,  
71 due to the absence of practical condition metrics that 1) have been validated against more sensitive  
72 biochemical indices, and 2) can be rapidly measured and analyzed in time to directly inform fisheries  
73 management decisions each fall.

74 Patterns of variability in energetic condition are often reflective of environmental conditions,  
75 food quantity and quality, and density dependence. While reductions in sea ice cover and warming in the  
76 Bering Sea are predicted to alter benthic-pelagic coupling and reduce energy available to benthic  
77 communities (Overland and Stabeno 2004; Grebmeier et al. 2006; Liovorn et al. 2016), our  
78 understanding of snow crab prey availability remains limited. Declines in juvenile snow crab body  
79 condition have been associated with warmer temperatures and declines in ice-associated diatom  
80 production in the Bering Sea, suggesting that temperature is an indirect driver of shifts in prey quality  
81 (Copeman et al. 2021). Likewise, evidence for climate-driven range contractions in snow crab points  
82 towards potential reductions in foraging area and prey availability as outcomes of warming (Fedewa et al.  
83 2020; Szwalski et al. 2023). Because population collapses can alter responses to environmental drivers  
84 (Durant et al. 2024), energetic responses to warming and record-high population density preceding the  
85 snow crab collapse may fundamentally differ from post-collapse responses when abundances are low.  
86 Elucidating the magnitude, direction and potential interactions between population density and  
87 temperature effects is critical in identifying drivers of collapse risk in the Bering Sea snow crab  
88 population.

89 To date, efforts to understand the snow crab collapse have solely focused on the eastern Bering  
90 Sea portion of the population despite support for high connectivity with snow crab in the northern Bering  
91 Sea (Ernst et al. 2005; Parada et al. 2010) Juvenile snow crab occupy a latitudinal gradient in the Bering  
92 Sea, with high densities extending northward into more consistently ice-covered areas of the northern

93 Bering Sea (north of ~60°N). The southern extent of their range is limited to shallow, cold-water habitats  
94 in the eastern Bering Sea (Murphy et al. 2010). While the largest magnitude of decline during the snow  
95 crab collapse occurred in juvenile nursery grounds in the eastern Bering Sea, the northern Bering Sea  
96 population also experienced declines in abundance coinciding with the 2018-2019 marine heatwave  
97 (Fedewa et al. 2020). However, sea ice loss and population declines in the north were less pronounced  
98 than in the eastern Bering Sea. This latitudinal population gradient and contrast in vulnerability to  
99 collapse provide a novel opportunity to compare energetic responses to population density and warming  
100 in collapsing and non-collapsing portions of the juvenile snow crab population during a marine heatwave.

101 The north-south latitudinal gradient in juvenile snow crab habitat and seasonal ice coverage also  
102 offers an opportunity to define optimal thermal habitat for snow crab by evaluating regional differences in  
103 energetic status across the full spatial extent of the Bering Sea. Anticipating the impacts of warming on  
104 thermal habitat suitability necessitates a better understanding of temperature effects on direct drivers of  
105 mortality risk such as energetic state. Bottom temperature appears to be an important predictor of snow  
106 crab habitat in the Bering Sea, and maximum thermal thresholds for snow crab have traditionally been  
107 defined as 2°C (Mueter and Litzow 2008; Murphy 2020). However, realized thermal niches likely differ  
108 in more consistently seasonally ice-covered habitat in the northern Bering Sea, and lower thermal  
109 preferences proposed for ice-associated species suggest that 1°C may be more biologically meaningful in  
110 delineating optimal thermal habitat for snow crab (Kotwicki and Lauth 2013). Furthermore, ecological  
111 insight into snow crab thermal preferences is critical for defining suitable habitat for population  
112 rebuilding, and predicting climate-mediated changes in habitat use and availability.

113 Here, we evaluate the role of energetics in collapse and recovery potential using a direct measure  
114 of energetic condition (i.e., total fatty acids in the hepatopancreas) applied across the collapsing (eastern)  
115 and non-collapsing (northern) portions of the Bering Sea snow crab population. Our specific objectives  
116 are to 1) test the hypothesis that energetic condition of juvenile snow crab covaries with population  
117 abundance during and after the collapse in the two regions; 2) test for regional differences in the

118 interactive effect of snow crab density and temperature on energetic condition; 3) use energetic condition  
119 to test for thermal optima that define suitable habitat for population recovery; and 4) evaluate an indirect  
120 condition metric (i.e., hepatopancreas percent dry weight) to allow routine rapid monitoring of energetic  
121 condition for early detection of future population declines. Ultimately, our approach will shed light on the  
122 causes and consequences of a mortality event underlying one of the largest marine invertebrate population  
123 collapses in recent history, and facilitate a better understanding of population recovery potential.

124 **MATERIALS AND METHODS**

125

126 *Study site and study population*

127 We collected hepatopancreas samples from juvenile snow crab (i.e., immature, pre-terminal molt  
128 individuals) across a latitudinal gradient on Alaska Fisheries Science Center Bering Sea bottom trawl  
129 surveys to allow for comparison of energetic condition in the northern and eastern portions of the Bering  
130 Sea continental shelf within the U.S. Exclusive Economic Zone. These two regions of the Bering Sea are  
131 targeted by separate bottom trawl surveys (annual in the eastern Bering Sea, biennial in the northern  
132 Bering Sea), and the fishery occurs exclusively in the eastern Bering Sea. Furthermore, these two  
133 portions of the snow crab population experienced different population trajectories following the extreme  
134 low-ice years of 2018-2019. Estimated snow crab abundance in the eastern Bering Sea reached a time  
135 series high in 2018 but declined more than 92% by 2021 (Fig. 1a). Abundance in the northern Bering Sea  
136 reached a similar high point in 2017 and declined 60% by 2021. In addition to the smaller proportional  
137 decline in the northern Bering Sea, this portion of the population showed a more rapid recovery, with  
138 abundance in 2022-2023 reaching 48-60% of the 2017 high point, while abundance in the eastern Bering  
139 Sea remained depressed until 2024 (Fig. 1a).

140

141

142

143 *Sampling design and data collection*

144 We sampled juvenile snow crab during the 2019 and 2021-2024 eastern Bering Sea bottom trawl  
145 surveys, and the 2019 and 2021-2023 northern Bering Sea bottom trawl surveys. The northern Bering Sea  
146 trawl survey was not conducted in 2024 following its transition to a biennial survey, and neither survey  
147 was conducted in 2020 due to the COVID-19 pandemic. The eastern Bering Sea bottom trawl survey  
148 occurs annually during May-July, with sampling conducted across 375 stations. The northern Bering Sea  
149 bottom trawl survey encompasses an additional 144 standardized stations that are sampled in August.  
150 Surveys in both regions utilize a systematic design (20 × 20 nautical mile grid) and an 83-112 Eastern  
151 bottom trawl (Stauffer 2004).

152

153 To ensure representative spatial coverage for energetics sampling in the two regions, we defined  
154 eight strata within the eastern and northern survey grids for stratified random sampling of juvenile snow  
155 crab habitat encompassing the middle and outer shelf of the Bering Sea. Stratum boundaries were  
156 delineated using marine regions developed by Ortiz et al. (2013), which are characterized by distinct  
157 ecological domains and oceanographic and bathymetric features. In each study year, we collected juvenile  
158 snow crab at a minimum of five survey stations within each stratum, aiming for a collection goal of 20  
159 male and 20 female snow crab per stratum (Table 1). We limited our collections to juvenile snow crab  
160 because energetic constraints on survival may be significantly more pronounced in juveniles as they  
161 undergo energetically costly molting events. Furthermore, baseline levels of total lipids and fatty acids  
162 vary with ontogeny and molt stage (Copeman et al. 2012), so we minimized potential age-based or  
163 ontological variability in our samples by employing minimum carapace width size thresholds to target  
164 pseudo-cohorts of newshell immature snow crab in the eastern Bering Sea ( $\geq 70$  mm carapace width  
165 males,  $\geq 45$  mm carapace width females) and the northern Bering Sea ( $\geq 50$  mm carapace width males,  $\geq$   
166 40 mm carapace width females). The size classes we targeted in the eastern Bering Sea portion of the  
167 population are expected to molt to maturity the following spring. Slightly smaller pseudo-cohorts were  
168 collected in the northern Bering Sea portion of the population because large immature snow crab are

169 encountered infrequently in this region due to smaller size at maturity (Divine et al. 2019) and directional  
170 northeast to southwest ontogenetic migrations (Ernst et al. 2005, Parada et al. 2010). Morphometric  
171 maturity in female snow crab was determined visually by assessing abdomen flap morphology (Jadamec  
172 et al. 1999). Male maturity was estimated with a distribution-based cutline approach that utilizes an  
173 allometric relationship between chela height and carapace width (Richar and Foy 2022). Specimen  
174 collections were conducted under permits from the Alaska Department of Fish and Game (permit  
175 numbers CF-19-032BT and CF-22-022BT).

176

177 *Modeling Covariates*

178 We estimated snow crab density at each station sampled by dividing the total number of all snow  
179 crab caught by area-swept effort (catch per unit effort; crab/nm<sup>2</sup>). Density estimates were right-skewed, so  
180 we fourth-root transformed CPUE data prior to use in statistical models to improve model fits. To  
181 compare snow crab population abundance trajectories in each region (Fig. 1a), we multiplied average  
182 snow crab density estimates across all survey stations within the respective eastern and northern Bering  
183 Sea survey grids by the survey grid area for each region. While our calculated abundance estimates do not  
184 implicitly account for poor survey gear selectivity of snow crab < 40 mm carapace width (Somerton et al.  
185 2013), abundance estimates are assumed to be a consistent measure of population size because selectivity  
186 is unlikely to have changed during our study period.

187

188 We measured bottom temperature at each station using a Sea-Bird SBE-39 datalogger (Sea-Bird  
189 Electronics Inc., Bellevue, WA) attached to the trawl headrope. Because summer bottom temperatures in  
190 the Bering Sea are significantly influenced by the maximum extent of spring sea ice, the timing of its  
191 retreat, and the formation of a cold, dense bottom-water layer (Stabeno et al. 2012), we also compared the  
192 magnitude of sea ice loss in the eastern and northern Bering Sea to characterize region-specific impacts of  
193 the 2018-2019 marine heatwave relative to our summer sampling efforts and estimates of energetic  
194 condition. To quantify sea ice loss, we plotted the spatial extent of average March sea ice concentration  $\geq$

195 15% using data from the ERA5 global reanalysis (Dee et al. 2011). This regional sea ice extent  
196 comparison shows that the eastern Bering Sea experienced a near-complete loss of sea ice in spring 2019,  
197 followed by the return of sea ice in 2021-2024, whereas the northern Bering Sea received at least partial  
198 ice coverage each spring (Fig. 1b).

199 *Energetic analyses*

200 Because the hepatopancreas is the primary energy storage organ in crustaceans, we collected  
201 hepatopancreas samples at sea for fatty acid analyses used to measure snow crab energetic condition.  
202 Snow crab were dissected on the survey vessel by opening the carapace and removing approximately 1g  
203 of hepatopancreas tissue from the body cavity, above the heart and gonads. Hepatopancreas samples were  
204 frozen at -40°C in sealed Eppendorf tubes wrapped in Teflon tape for three to six months prior to  
205 processing. To measure hepatopancreas percent dry weight (i.e. indirect energetic condition metric),  
206 samples were briefly thawed and rigorously mixed to a homogeneous consistency.

207  $(\pm 0.001 \text{ g})$

208 pre-weighed aluminum tray, drying at 65 °C for 72 hours to a constant mass, and then weighing to  
209 determine the dry weight (DWT, g).

210

211 To measure total fatty acid concentration (i.e. direct energetic condition metric), we used a 100  
212 mg sample of wet hepatopancreas. Tissues were weighed (approx.  $100 \pm 0.001 \text{ mg}$ ) into lipid-cleaned 15  
213 mL thick-walled glass tubes with Teflon-lined screw caps. An internal standard (23:0 methyl ester) was  
214 added at 10% of the estimated total fatty acid weight. We dried internal standards and hepatopancreas  
215 tissues under a steady stream of nitrogen gas until all visible moisture was removed from the sample.  
216 Fatty acid methyl esters (FAME) were synthesized using a rapid one-step acid-catalyzed direct extraction  
217 and methylation procedure. Following Meier et al. (2006), 1 ml of anhydrous methanol containing 2.5M  
218 HCl was added to tissue samples and derivatized. Select samples were checked to assure complete  
219 derivatization of lipids to FAMEs using thin-layer chromatography with flame ionization detection  
220 (TLC\_FID) on a Mark VI Iatroskan (Copeman et al. 2021). Quantitative FAME measures were

221 determined using gas chromatography with flame ionization detection (GC-FID) on a HP 7890 GC-FID  
222 equipped with an autosampler and a DB wax + GC column (Agilent Technologies, Inc., U.S.A.). The  
223 column was 30 m in length, the internal diameter was 0.25 mm and the column film thickness was 0.25  
224  $\mu\text{m}$ . The oven temperature began at 65°C and was held at this temperature for 0.5 min. Oven temperature  
225 was increased to 195°C (40°C/min), held for 15 min then increased again (2 °C/min) to a final  
226 temperature of 220°C, which was held for 1 min. The hydrogen carrier gas flowed at a rate of 2 ml/min  
227 and the injector and detector temperatures were set at 250°C. Peaks were identified using retention times  
228 based upon standards purchased from Supelco (37 component FAME, BAME, PUFA 1, PUFA 3).  
229 Chromatograms were integrated using Chem Station (version A.01.02, Agilent). Total fatty acid  
230 concentration in the hepatopancreas was expressed as either total fatty acids (mg) per wet weight (WWT,  
231 g) or dry weight (DWT, g).

232

### 233 *Data analyses*

234 *Objective 1: Covariation between energetic condition and snow crab abundance.* To evaluate evidence  
235 for regional variation in energetic condition during and after the snow crab collapse, we used Bayesian  
236 hierarchical regression models to generate annual estimates of mean energetic condition and 95% credible  
237 intervals for the collapsing (eastern) and non-collapsing (northern) portions of the population. We began  
238 by estimating annual mean energetic condition and uncertainty for each region to compare time series of  
239 energetic status for the two portions of the population. These estimates were generated using separate  
240 models for each region, since we were not interested in sharing information across regions. The model for  
241 each region took the form:

$$242 Y_{t,i,j,s} = \beta_0 + \beta_1 YEAR_t + f_1(SIZE_s) + f_2(DOY_{t,i}) + \alpha STRATUM_j + \varepsilon_{t,i,j,s} \quad (1)$$

243 where  $Y_{t,i,j,s}$  is the total fatty acids per wet weight estimate for a snow crab sampled in year  $t$  at station  $i$  in  
244 stratum  $j$  at size  $s$ ,  $\beta_0$  is the intercept, YEAR is a categorical population-level (fixed) effect,  $f_1$  is a smooth  
245 function of crab carapace width (SIZE),  $f_2$  is a smooth function of the Julian day at which station  $i$  was  
246 sampled in year  $t$  (day of year, DOY),  $\alpha_j$  is a group-level (random) effect to account for spatial

247 autocorrelation of samples collected within sampling stratum  $j$ , and  $\varepsilon_{t,i,j,s}$  is the individual-level residual  
248 error. We included snow crab carapace width and sampling day as control variables to account for  
249 potentially confounding influences of seasonality and ontogeny on our energetic condition estimates.  
250 Non-linear relationships were accounted for in the effect of continuous variables (i.e., crab size and  
251 sampling day) using thin plate regression splines, and smooths were limited to three basis functions to  
252 avoid overfitting. Models utilized a zero-truncated Gaussian response distribution and flat priors.

253  
254 Next, we used these model-derived annual estimates of energetic condition to support a  
255 comparative analysis between energetic condition and population change to assess whether stronger and  
256 more persistent declines in abundance in the collapsing eastern Bering Sea covaried with declines in  
257 energetic condition. Our study design provides a dataset spanning five years and two regions, which we  
258 judged as too small to support a robust regression-based analysis of region-specific energetic condition at  
259 an annual scale. Accordingly, we used the annual energetic condition estimates produced from region-  
260 specific regression models (Eq. 1) and compared these to eastern and northern Bering Sea snow crab  
261 population-level abundance estimates derived from the full survey grid for each respective region (Fig.  
262 1a) to qualitatively assess for covariation (i.e., synchronous changes in the direction of abundance and  
263 energetic condition estimates).

264  
265 *Objective 2: Interactive effects of population density and temperature.* To evaluate evidence for an  
266 interactive effect of population density and bottom temperature on energetic condition, and to test  
267 whether the strength and direction of this interaction differed between the collapsing and non-collapsing  
268 portions of the snow crab population, we fit a single Bering Sea-wide Bayesian regression model that  
269 pooled energetic condition estimates across both regions. The full model took the form:

$$270 \quad Y_{t,i,j,s} = \beta_0 + \beta_1(CPUE_{t,i}, TEMP_{t,i}, REGION) + f_1(SIZE_s) + f_2(DOY_{t,i}) + \alpha STRATUM_j + \varepsilon_{t,i,j,s} \quad (2)$$

272 where  $Y_{t,i,j,s}$  is the total fatty acids per wet weight estimate for a snow crab sampled in year  $t$  at station  $i$  in  
273 stratum  $j$  at size  $s$ ,  $\beta_0$  is the intercept, CPUE is the population-level snow crab density at station  $i$  sampled  
274 in year  $t$  that interacts with bottom temperature at station  $i$  sampled in year  $t$  (TEMP) and the Bering Sea  
275 region (REGION),  $f_1$  is a smooth function of crab carapace width (SIZE),  $f_2$  is a smooth function of the  
276 Julian day at which station  $i$  was sampled in year  $t$  (day of year, DOY),  $\alpha_j$  is a group-level (random) effect  
277 to account for spatial autocorrelation of samples collected within sampling stratum  $j$ , and  $\varepsilon_{t,i,j,s}$  is the  
278 individual-level residual error. The full model was fit using a zero-truncated Gaussian response  
279 distribution and flat priors, and smooths were limited to three basis functions to avoid overfitting. We  
280 evaluated model performance and out-of-sample predictive skill with the Bayes  $R^2$  (Gelman et al. 2019).

281

282 *Objective 3: Defining optimal thermal habitat.* If there was support for an interaction between  
283 temperature and density, we used the Bering Sea-wide regression model (Eq. 2) to evaluate the effect of  
284 density dependence on energetic condition at a representative range of temperatures. We *a priori* defined  
285 four representative bottom temperature values (0°, 1°, 2°, and 3°C) based on previous research, and  
286 evaluated the conditional effects of the density  $\times$  temperature interaction on energetic condition of  
287 collapsing and non-collapsing portions of the population at these four temperature values. This approach  
288 enabled us to determine the relative energetic consequences of changes in density and temperature, and to  
289 define thermal habitat optima that may promote population recovery.

290

291 *Objective 4. Evaluating an indirect condition metric.* To assess the predictive accuracy of  
292 hepatopancreas percent dry weight as a rapid, indirect metric to monitor energetic condition, we used a  
293 Bayesian regression model to evaluate the relationship between hepatopancreas percent dry weight and  
294 hepatopancreas total fatty acid concentration per dry weight of individual snow crab samples with paired  
295 measurements. For this analysis, we fit data from 2021 to 2024 at-sea collections, pooling eastern and  
296 northern Bering Sea samples ( $n = 974$ ). The regression model was fit using a Gaussian response  
297 distribution and flat priors.

298  
299 All Bayesian analyses were conducted in the Stan computational framework (Stan Development  
300 Team 2024) and implemented in the 'brms' package (Bürkner et al. 2017) in R v4.4.2 (R Core Team  
301 We conducted estimation with four parallel MCMC chains and 10,000 iterations. Chain  
302 convergence and model fits were examined using the potential scale reduction factor ( $\hat{R} < 1.05$ ), effective  
303 sample sizes, Leave One Out Probability Integral Transform (LOO-PIT) plots, simulated DHARMA  
304 residual plots (Hartig and Hartig 2017) and posterior predictive checks (Gabry et al. 2019; Gelman et al.  
305 2020). We also investigated the sensitivity of the posterior to perturbations of the prior and likelihood to  
306 diagnose any prior-data conflicts (Kallioinen et al. 2023). Posterior summaries (means and 80/90/95%  
307 credible intervals) of conditional effects were estimated to compare energetic condition across collapsing  
308 and non-collapsing portions of the population, and  
309 temperature and density effects on energetic condition.

310

## 311 RESULTS

312 Overall, a total of 1,325 juvenile snow crab hepatopancreas samples were collected from mid-  
313 June to mid-August during the 2019-2024 eastern and northern Bering Sea surveys. Sampled snow crab  
314 ranged in size from 40.16 to 113.2 mm carapace width. Over the five-year sampling period, trajectories of  
315 snow crab density and bottom temperature at sampled stations differed substantially between the eastern  
316 and northern Bering Sea. The collapsing eastern Bering Sea portion of the population showed an 84%  
317 decline in mean density from 2019 to 2021 (Fig. 2a). In contrast, density in the non-collapsing northern  
318 Bering Sea portion of the population remained, on average, nearly four times higher than density in the  
319 collapsing portion of the population from 2021 to 2023. However, the eastern Bering Sea portion of the  
320 population showed a possible sign of recovery in 2024, with density increasing over 10-fold from 2023 to  
321 2024. Average bottom temperatures in the eastern Bering Sea exceeded 3°C in 2019, while the northern  
322 Bering Sea average bottom temperature remained below 1.5°C during the study period (Fig. 2b).

323

324

325 *Covariation between energetic condition and population change*

326 The posterior means estimated from our region-specific eastern and northern Bering Sea models  
327 indicate substantial interannual variability in energetic condition in the collapsing (eastern) portion of the  
328 population, as evidenced by nonoverlapping 95% credible intervals (Fig. 3). Furthermore, changes in  
329 energetic condition in the two regions reflected differences in population trajectories between the  
330 collapsing and non-collapsing portions of the population. Mid-collapse (2019), eastern Bering Sea snow  
331 crab mean energetic condition fell to 51 mg FA/g WWT (95% credible interval [CI] = 36-73 mg fatty  
332 acid /g WWT), a 49-63% decrease relative to posterior means in years following the collapse (101-139  
333 mg fatty acid/g WWT; Fig. 3). Furthermore, a post-collapse increase in energetic condition coincided  
334 with substantial increases in eastern Bering Sea snow crab abundance from 2021 to 2024. In contrast,  
335 annual estimates of energetic condition were more constant in the non-collapsing northern portion of the  
336 population, and mean energetic condition never fell below 80 mg fatty acid/g WWT during the study  
337 period (Fig. 3).

338

339 *Interactive effects of population density and temperature.*

340 The Bering Sea-wide model showed clear support for interactive effects of population density and  
341 temperature that differed between the collapsing and non-collapsing portions of the population (density x  
342 temperature x region interaction estimate = 1.44, 95% CI = [0.60, 2.29]). Specifically, we found strong  
343 support for a negative interaction between temperature and population density on energetic condition in  
344 the collapsing portion of the population. Plots of posterior density effects for the collapsing region at four  
345 representative temperatures (0°, 1°, 2°, and 3°C) showed negative effects of snow crab density at warmer  
346 temperatures (1°C-3°C) and a neutral effect of snow crab density at 0°C (Fig. 4a). In contrast, we did not  
347 find support for an interactive effect of temperature and population density on energetic condition in the  
348 non-collapsing portion of the population. Instead, posterior density effects at all four temperature levels  
349 for the non-collapsing region could not be distinguished from a zero-slope line, and energetic condition

350 remained stable at high densities and high temperatures (Fig. 4b). We also observed a seasonal increase in  
351 energetic condition from mid-June to early August (Fig. S1a), and found no evidence for a crab size effect  
352 (i.e., the effect could not be distinguished from a zero-slope line; Fig. S1b). The Bering Sea-wide model  
353 for energetic condition across collapsing and non-collapsing portions of the snow crab population  
354 returned a Bayesian  $R^2 = 0.17$ . This relatively low proportion of variance explained is likely due to the  
355 inclusion of northern Bering Sea data that showed weak responses to model covariates, whereas a reduced  
356 version of the model fit only to eastern Bering Sea samples explained roughly a quarter of variance  
357 (Bayesian  $R^2 = 0.24$ ).

358

### 359 *Performance of a rapid condition metric*

360 We found that the proposed rapid metric was a good predictor of energetic condition, supported  
361 by a strong positive relationship between hepatopancreas percent dry weight and total fatty acid  
362 concentration (mg/g DWT) across the four years of data (Fig. 5). Percent dry weight of the  
363 hepatopancreas explained 64% of the variation in hepatopancreas total fatty acids. The strength of this  
364 relationship was consistent among sampling years and regions, indicating strong predictive ability of  
365 hepatopancreas percent dry weight as an indicator of energetic reserves in juvenile snow crab.

## 366 DISCUSSION

367 Population collapses are often associated with low rates of recovery (Hutchings and Reynolds  
368 2004), highlighting the need for improved understanding of factors associated with persistent population  
369 decline and recovery potential. Here, we used a direct measure of energetic condition in juvenile snow  
370 crab to demonstrate empirical linkages between energetic reserves and collapse and population recovery  
371 trajectories. Synchronous declines in energetic condition and abundance in the collapsing portion of the  
372 Bering Sea snow crab population point to energetic limitations during a marine heatwave as a proximate  
373 mechanism for increased mortality and population collapse. While our study adds to the growing  
374 evidence linking poor energetic condition to marine population collapses (e.g. Dutil and Lambert 2000;

375 Sherwood et al. 2007; Barbeaux et al. 2020), our results provide novel insights into collapse risk and  
376 vulnerability to warming. We demonstrate that the non-collapsing, northern portion of the snow crab  
377 population maintained relatively stable energetic condition associated with a reduced magnitude of  
378 warming during the 2018-2019 marine heatwave relative to the eastern Bering Sea. We also show that  
379 energetic condition rebounded rapidly in the eastern Bering Sea portion of the population following the  
380 collapse and marine heatwave. This finding, coinciding with strong recruitment and increasing population  
381 abundance from 2021 to 2024 in the eastern Bering Sea (Fig. 1a), demonstrates support for initial  
382 population recovery post-collapse. Likewise,

383 suggests that the snow crab collapse may be reversible when the ecosystem returns to pre-  
384 heatwave conditions. While initial recovery appears to be relatively rapid compared to collapses in other  
385 species (Hutchings 2000; Neubauer et al. 2013), our results emphasize that successful recruitment to the  
386 fishable portion of the snow crab population is critically dependent on conditions that promote increased  
387 energetic condition and survival of juveniles. Our study is the first to provide critical perspectives on  
388 region-specific energetic outcomes through the inclusion of the non-collapsing portion of the snow crab  
389 population, and our results highlight how this comparative approach can improve our understanding of  
390 collapse and recovery dynamics.

391 We attributed declines in energetic condition in the collapsing portion of the population to a  
392 strong negative interaction between elevated bottom temperatures and high population density, and we  
393 found that temperature mediates the direction and magnitude of density-dependent effects on energetic  
394 condition. The ecological interaction detected in our study underscores the energetic consequences  
395 associated with the combination of high snow crab density and bottom temperatures  $\geq 1^{\circ}\text{C}$ . We also show  
396 that cold-water habitat ( $\leq 0^{\circ}\text{C}$ ) in the eastern Bering Sea is critical for sustaining high snow crab densities  
397 consistent with rebuilding and population recovery. This result is supported by the understanding that  
398 snow crab are highly stenothermic and critically reliant on cold temperatures (Dionne et al. 2003).  
399 However, our results highlight that an additive interpretation of temperature and density effects on snow

400 crab is inappropriate, as the strength of density-dependent processes was highly influenced by bottom  
401 temperature and the effect may, instead, be synergistic. While high population density and unusually  
402 warm bottom temperatures have previously been linked to the eastern Bering Sea snow crab collapse  
403 (Szuwalski et al. 2023), our approach revealed that energetic responses to density and temperature effects  
404 differed regionally between collapsing and non-collapsing portions of the snow crab population. We  
405 found no support for interactive effects on energetic condition in the non-collapsing portion of the  
406 population to the north, where our results suggest that juvenile snow crab are able to maintain energetic  
407 reserves across the full range of temperatures and population densities observed in the northern Bering  
408 Sea during our study period. Strong benthic-pelagic coupling and carbon flux to the benthos have  
409 historically supported high macrofaunal biomass in the northern Bering Sea (Grebmeier et al. 1988),  
410 suggesting that ample benthic prey resources may buffer juvenile snow crab from potential declines in  
411 energetic condition despite increased metabolic demand at higher temperatures. Conversely, high  
412 population densities and extreme temperatures in the collapsing portion of the population may require  
413 snow crab to utilize energetic reserves to offset density-dependent reductions in prey availability and  
414 thermally-driven increases in metabolic rates. However, we caution that our conclusion supporting  
415 interactive density and temperature effects is based on a limited set of observations in our study period. In  
416 particular, energetic responses have not yet been observed under a combination of high temperatures and  
417 low densities in the collapsing portion of the population.

418 Past studies have defined snow crab thermal habitat preferences in the Bering Sea using  
419 presence/absence or abundance data derived from fishery-independent surveys (Murphy 2020; Fedewa et  
420 al. 2020), although these approaches lack causal mechanisms. We improve on this limitation by utilizing  
421 energetic condition as a proximate mechanism for survival to demonstrate that temperatures  $\leq 0^{\circ}\text{C}$  are  
422 more meaningful in defining optimal thermal habitat for high-density juvenile snow crab nurseries than  
423 previously-defined 2-3 $^{\circ}\text{C}$  Bering Sea thresholds (Litzow and Mueter 2008; Murphy 2020). Similarly, the  
424 cold intermediate layer (CIL) in Atlantic Canada, defined as waters below 0 $^{\circ}\text{C}$ , is closely associated with

425 snow crab spatial distributions and habitat (Dionne et al. 2003), lending support to our findings. However,  
426 this 0°C temperature optimum appears to be biologically meaningful to the collapsing portion of the snow  
427 crab population only, and we found evidence for a larger realized thermal niche in the non-collapsing  
428 portion of the population. While laboratory studies indicate that thermal tolerances were likely not  
429 exceeded during the 2018-2019 marine heatwave (Foyle 1989), laboratory conditions often poorly predict  
430 realized thermal niches. Our study, instead, highlights the importance of conspecific density, availability  
431 of bottom waters  $\leq 0^{\circ}\text{C}$ , and energetic status when defining thermal preferences for Bering Sea snow  
432 crab.

433 Despite the strengths of our approach, a direct mechanism for regionally-varying thermal  
434 responses observed in this study remains unclear. Declines in eastern Bering Sea snow crab abundance  
435 during the marine heatwave were driven by a broader ecosystem transition from Arctic to boreal  
436 conditions, and an index of this ecosystem reorganization outperformed bottom temperatures alone as a  
437 predictor of declining snow crab abundance (Litzow et al. 2024). This result, combined with illustrated  
438 linkages between snow crab productivity and both sea ice extent and large-scale climate indices  
439 (Szuwalski et al. 2020; Mullowney et al. 2023), suggest that invoking temperature as a mechanistic driver  
440 for shifts in energetic condition likely oversimplifies complex ecosystem responses linked to spring sea  
441 ice dynamics and food availability to the benthos (Copeman et al. 2025). Given that the northern Bering  
442 Sea has not yet reached environmental extremes evidenced in the eastern Bering Sea in recent decades  
443 (Stabeno and Bell 2019; Overland et al. 2024) and spring sea ice covered the majority of snow crab  
444 habitat in the northern Bering Sea during the marine heatwave (Fig. 1b), we propose that the presence of  
445 spring sea ice may mediate the negative consequences of elevated temperatures and high population  
446 density that impacted the collapsing portion of the population to the south. This idea is further supported  
447 by findings that minimum sea ice extent thresholds drive shifts in the northern Bering Sea zooplankton  
448 community (Kimmel et al. 2023) and the prevalence of open-water spring phytoplankton blooms (Nielsen  
449 et al. 2024), which collectively influence the availability of basal resources to the benthos. Taken

450 together, these results emphasize that continued warming and loss of sea ice in the northern Bering Sea  
451 may reveal temperature thresholds and critical tipping points in the non-collapsing portion of the  
452 population as this system continues to encounter conditions that are outside the envelope of historic  
453 observations.

454 Rapid warming in the Bering Sea poses a pressing challenge to fisheries management, and  
455 decision makers are increasingly reliant on real-time indicators of ecosystem and population conditions to  
456 capture shifts in stock productivity (Caddy 2004). Here, we present a rapid indirect measure of energetic  
457 condition (i.e., percent dry weight of the hepatopancreas) that effectively tracks bottom-up effects on  
458 snow crab productivity, and accurately predicts direct biochemical energetic condition measurements that  
459 are highly sensitive to environmental change in the Bering Sea. Our results also highlight the utility of a  
460 rapid energetic condition metric that effectively replaces time-intensive and cost-prohibitive biochemical  
461 analyses that can delay the uptake of energetics data. While percent dry weight of the hepatopancreas has  
462 previously been utilized to estimate energetic condition in laboratory-reared snow crab (Hardy et al. 2000;  
463 Godbout et al. 2002), we are unaware of any efforts to date that have employed this metric annually to  
464 provide a rapid health assessment for monitoring snow crab populations. Co-varying energetic condition  
465 and population abundance trajectories in this study suggest that our validated rapid energetic condition  
466 metric can provide inference about likely population trends, thus providing strong support for operational  
467 use in fisheries management. The recent development and integration of stock-specific Ecosystem and  
468 Socioeconomic Profiles (Shotwell et al. 2023) and risk tables (Dorn and Zador 2020) into the North  
469 Pacific Fishery Management Council decision-making process provides a mechanism for direct  
470 integration of our rapid condition metric into Bering Sea crab management decisions, and supports  
471 approaches to ecosystem-based fisheries management (Kruse et al. 2025).

472 Our work highlights the importance of continued field collections and energetic-based monitoring  
473 to facilitate a more robust exploration of mechanistic relationships between energetics, sea ice dynamics,  
474 and population outcomes, which are critical to developing skillful forecasts of collapse potential and

475 climate change impacts. While we consider our energetics dataset to be highly effective in tracking  
476 population trajectories in Bering Sea snow crab, our results are inherently limited in scope due to our  
477 short observation period (five years). Our models explained a fairly low amount of variation in energetic  
478 condition estimates, suggesting that future efforts should focus on elucidating direct drivers of energetic  
479 condition such as prey quantity and quality. Furthermore, while there is strong evidence that depleted  
480 hepatopancreas lipid stores are indicative of starvation-induced mortality in snow crab (Hardy et al.  
481 2000), groundtruthoring our field-collected measures of energetic condition with demographic outcomes in  
482 laboratory experiments is a necessary next step to determine critical energetic thresholds and  
483 physiological tipping points for survival (Lambert and Dutil 1997; Dutil and Lambert 2000). Such  
484 applications would facilitate the development of operational, condition-corrected natural mortality rates  
485 for direct incorporation into stock assessments (Casini et al. 2016; Regular et al. 2022; Björnsson et al.  
486 2022), or provide a mechanistic basis for time-varying natural mortality estimates (Szuwalski 2022).  
487 Despite these limitations, our findings highlight important advances in the understanding of collapse and  
488 recovery dynamics, and we anticipate that our empirical approach and development of a rapid energetic  
489 condition metric will improve the ability to detect impending population collapses.

490

491 **Acknowledgements:** We would like to thank Michelle Stowell, Samantha Mundorff, Michele Ottmar,  
492 Emily Vernon, and Joletta Silva for assistance with sample processing and laboratory analyses. We thank  
493 scientists and crew on the FV Alaska Knight, FV Vesteraalen and FV Northwest Explorer for assistance  
494 with at-sea sample collection on the eastern and northern Bering Sea bottom trawl surveys. Comments  
495 provided by L. Zacher, C. Szuwalski, M. Olmos, A. Favreau and three anonymous reviewers helped  
496 improve this manuscript. The findings and conclusions in this paper are those of the authors and do not  
497 necessarily represent the views of the National Marine Fisheries Service, NOAA. Reference to trade  
498 names does not imply endorsement from the National Marine Fisheries Service, NOAA.

499

500  
501 **Competing Interests Statement:** The authors declare there are no competing interests.  
502  
503 **Author Contribution Statement:** **EJF:** Conceptualization, Funding acquisition, Investigation,  
504 Visualization, Methodology, Formal analysis, Writing - original draft, Writing - review & editing, **LAC:**  
505 Conceptualization, Funding acquisition, Investigation, Methodology, Writing - original draft, Writing -  
506 review & editing, **MAL:** Methodology, Formal analysis, Writing - original draft, Writing - review &  
507 editing  
508  
509 **Funding Statement:** This research was supported through the North Pacific Research Board,  
510 [www.nprb.org](http://www.nprb.org); NPRB Core Project Number 1911.  
511  
512 **Data Availability Statement:** Raw data, metadata and R code for reproducing all analyses are publicly  
513 available on Zenodo (DOI: 10.5281/zenodo.17246422).  
514  
515  
516  
517  
518  
519  
520  
521

522 **References**

523 Barbeaux, S.J., Holsman, K., and Zador, S. 2020. Marine heatwave stress test of ecosystem-based  
524 fisheries management in the Gulf of Alaska Pacific cod fishery. *Front. Mar. Sci.* 7: 703.  
525 doi:10.3389/fmars.2020.00703.

526 Björnsson, B., Sólmundsson, J., and Woods, P.J. 2022. Natural mortality in exploited fish stocks: annual  
527 variation estimated with data from trawl surveys. *ICES J. Mar. Sci.* 79(5): 1569-1582.  
528 doi:10.1093/icesjms/fsac063.

529 Bürkner, P-C. 2017. brms: An R package for Bayesian Multilevel Models using Stan. *J. Stat. Software*  
530 80(1): 1 - 28. doi:10.18637/jss.v080.i01.

531 Caddy, J.F. 2004. Current usage of fisheries indicators and reference points, and their potential  
532 application to management of fisheries for marine invertebrates. *Can. J. Fish. Aquat. Sci.* 61(8):  
533 1307-1324. doi:10.1139/f04-132.

534 Carvalho, K.S., Smith, T.E., and Wang, S. 2021. Bering Sea marine heatwaves: Patterns, trends and  
535 connections with the Arctic. *Journal of Hydrology* 600: 126462.  
536 doi:<https://doi.org/10.1016/j.jhydrol.2021.126462>.

537 Casini, M., Eero, M., Carlshamre, S., and Lövgren, J. 2016. Using alternative biological information in stock assessment: condition-corrected  
538 natural mortality of Eastern Baltic cod. *ICES Journal of Marine Science* 73(10): 2625-2631.  
539 doi:10.1093/icesjms/fsw117.

540 Copeman, L.A., Stoner, A.W., Ottmar, M.L., Daly, B., Parrish, C.C., and Eckert, G.L. 2012. Total lipids,  
541 lipid classes, and fatty acids of newly settled red king crab (*Paralithodes camtschaticus*):  
542 comparison of hatchery-cultured and wild crabs. *J. Shellfish Res.* 31(1): 153-165.  
543 doi:10.2983/035.031.0119.

544 Copeman, L., Ryer, C., Spencer, M., Ottmar, M., Iseri, P., Sremba, A., Wells, J., and Parrish, C. 2018.  
545 Benthic enrichment by diatom-sourced lipid promotes growth and condition in juvenile Tanner  
546 crabs around Kodiak Island, Alaska. *Mar. Ecol. Progr. Ser.* 597: 161-178.

547 Copeman, L.A., Ryer, C.H., Eisner, L.B., Nielsen, J.M., Spencer, M.L., Iseri, P.J., and Ottmar, M.L.  
548 2021. Decreased lipid storage in juvenile Bering Sea crabs (*Chionoecetes* spp.) in a warm (2014)  
549 compared to a cold (2012) year on the southeastern Bering Sea. *Polar Biol.* 44(9): 1883-1901.  
550 doi:10.1007/s00300-021-02926-0.

551 Copeman, L.A., Mundorff, S.M., Ottmar, M.L., Stowell, M.A., and Spencer, M.L. 2025. Temperature  
552 affects growth rates while dietary lipid influences condition metrics in juvenile Tanner crab  
553 (*Chionoecetes bairdi*). *J Exp Mar Biol Ecol* 588: 152105.  
554 doi:<https://doi.org/10.1016/j.jembe.2025.152105>.

555 Dee, D.P., Uppala, S.M., Simmons, A.J., Berrisford, P., Poli, P., Kobayashi, S., Andrae, U., Balmaseda,  
556 M.A., Balsamo, G., Bauer, P., Bechtold, P., Beljaars, A.C.M., van de Berg, L., Bidlot, J.,  
557 Bormann, N., Delsol, C., Dragani, R., Fuentes, M., Geer, A.J., Haimberger, L., Healy, S.B.,  
558 Hersbach, H., Hölm, E.V., Isaksen, L., Källberg, P., Köhler, M., Matricardi, M., McNally, A.P.,  
559 Monge-Sanz, B.M., Morcrette, J.-J., Park, B.-K., Peubey, C., de Rosnay, P., Tavolato, C.,  
560 Thépaut, J.-N., and Vitart, F. 2011. The ERA-Interim reanalysis: configuration and performance  
561 of the data assimilation system. *Q. J. Royal Meteorol. Soc.* 137(656): 553-597.  
562 doi:10.1002/qj.828.

563 Dionne, M., Sainte-Marie, B., Bourget, E., and Gilbert, D. 2003. Distribution and habitat selection of  
564 early benthic stages of snow crab *Chionoecetes opilio*. *Mar. Ecol. Progr. Ser.* 259: 117-128.

565 Divine, L.M., Mueter, F.J., Kruse, G.H., Bluhm, B.A., Jewett, S.C., and Iken, K. 2019. New estimates of  
566 weight-at-size, maturity-at-size, fecundity, and biomass of snow crab, *Chionoecetes opilio*, in the  
567 Arctic Ocean off Alaska. *Fisheries Research* 218: 246-258.  
568 doi:<https://doi.org/10.1016/j.fishres.2019.05.002>.

569 Dorn, M.W., and Zador, S.G. 2020. A risk table to address concerns external to stock assessments when  
570 developing fisheries harvest recommendations. *Ecosyst. Health Sustain.* 6(1): 1813634.  
571 doi:10.1080/20964129.2020.1813634.

572 Durant, J.M., Holt, R.E., and Langangen, Ø. 2024. Large biomass reduction effect on the relative role of  
573 climate, fishing, and recruitment on fish population dynamics. *Sci. Rep.* 14(1): 8995.  
574 doi:10.1038/s41598-024-59569-4.

575 Dutil, J.D., and Lambert, Y. 2000. Natural mortality from poor condition in Atlantic cod (*Gadus morhua*).  
576 *Can. J. Fish. Aquat. Sci.* 57(4): 826-836. doi: 10.1139/cjfas-57-4-826.

577 Ernst, B., Orensanz, J., and Armstrong, D. 2005. Spatial dynamics of female snow crab (*Chionoecetes*  
578 *opilio*) in the eastern Bering Sea. *Canadian Journal of Fisheries and Aquatic Sciences* 62(2): 250-  
579 268.

580 Fedewa, E.J., Jackson, T.M., Richar, J.I., Gardner, J.L., and Litzow, M.A. 2020. Recent shifts in northern  
581 Bering Sea snow crab (*Chionoecetes opilio*) size structure and the potential role of climate-  
582 mediated range contraction. *Deep-Sea Res. Pt. II Top. Stud. Oceanogr.* 181: 11.  
583 doi:10.1016/j.dsr2.2020.104878.

584 Fey, S.B., Siepielski, A.M., Nusslé, S., Cervantes-Yoshida, K., Hwan, J.L., Huber, E.R., Fey, M.J.,  
585 Catenazzi, A., and Carlson, S.M. 2015. Recent shifts in the occurrence, cause, and magnitude of  
586 animal mass mortality events. *Proc. Nat. Acad. Sci.* 112(4): 1083-1088.  
587 doi:10.1073/pnas.1414894112.

588 Foyle, T.P., Odor, R.K., and Elner, R.W. 1989. Energetically defining the thermal limits of the snow crab.  
589 *J. Exp. Biol.* 145: 371-393.

590 Gabry, J., Simpson, D., Vehtari, A., Betancourt, M., and Gelman, A. 2019. Visualization in Bayesian  
591 workflow. *J. Royal Stat. Soc. Ser. A: Stat. Soc.* 182(2): 389-402. doi:10.1111/rssa.12378.

592 Gelman, A., Goodrich, B., Gabry, J., and Vehtari, A. 2019. R-squared for Bayesian regression models.  
593 *Am. Stat.* 73(3): 307-309.

594 Gelman, A., Vehtari, A., Simpson, D., Margossian, C.C., Carpenter, B., Yao, Y., Kennedy, L., Gabry, J.,  
595 Bürkner, P.-C., and Modrák, M. 2020. Bayesian Workflow. *arXiv:2011.01808*.

596 Godbout, G., Dutil, J.-D., Hardy, D., and Munro, J. 2002. Growth and condition of post-moult male snow  
597 crab (*Chionoecetes opilio*) in the laboratory. *Aquaculture* 206(3): 323-340

598 Grebmeier, J.M., McRoy, C.P., and Feder, H.M. 1988. Pelagic-benthic coupling on the shelf of the  
599 northern Bering and Chukchi seas. 1. Food-supply source and benthic biomass. *Mar. Ecol. Progr. Ser.* 48(1): 57-67. doi:10.3354/meps048057.

600 Grebmeier, J.M., Overland, J.E., Moore, S.E., Farley, E.V., Carmack, E.C., Cooper, L.W., Frey, K.E.,  
601 Helle, J.H., McLaughlin, F.A., and McNutt, S.L. 2006. A major ecosystem shift in the northern  
602 Bering Sea. *Science* 311(5766): 1461-1464. doi:10.1126/science.1121365.

603 Hardy, D., Dutil, J.-D., Godbout, G., and Munro, J. 2000. Survival and condition of hard shell male adult  
604 snow crabs (*Chionoecetes opilio*) during fasting at different temperatures. *Aquaculture* 189(3-4):  
605 259-275.

606 Hartig, F., and Hartig, M.F. 2017. Package ‘dharma’. R package 531: 532.

607 Hobday, A.J., Alexander, L.V., Perkins, S.E., Smale, D.A., Straub, S.C., Oliver, E.C.J., Benthuysen, J.A.,  
608 Burrows, M.T., Donat, M.G., Feng, M., Holbrook, N.J., Moore, P.J., Scannell, H.A., Sen Gupta,  
609 A., and Wernberg, T. 2016. A hierarchical approach to defining marine heatwaves. *Prog  
610 Oceanogr* 141: 227-238. doi:<https://doi.org/10.1016/j.pocean.2015.12.014>.

611 Hutchings, J. 2000. Collapse and recovery of marine fishes. *Nature* 406: 882-885.  
612 doi:10.1038/35022565.

613 Hutchings, J.A., and Reynolds, J.D. 2004. Marine fish population collapses: consequences for recovery  
614 and extinction risk. *BioScience* 54(4): 297-309.  
615 doi:10.1641/0006568(2004)054[0297:Mfpccf]2.0.Co;2.

617 Jadamec, L., Donaldson, W., and Cullenberg, P. 1999. Biological field techniques for *Chionoecetes* crabs.  
618 University of Alaska Sea Grant AK-SG-99-02, Fairbanks, AK.

619 Kallioinen, N., Paananen, T., Bürkner, P-C., and Vehtari, A. 2023. Detecting and diagnosing prior and  
620 likelihood sensitivity with power-scaling. *Stat. Comput.* 34(1): 57. doi:10.1007/s11222-023-  
621 10366-5.

622 Kimmel, D.G., Eisner, L.B., and Pinchuk, A.I. 2023. The northern Bering Sea zooplankton community  
623 response to variability in sea ice: evidence from a series of warm and cold periods. *Mar Ecol  
624 Prog Ser* 705: 21-42. doi:10.3354/meps14237.

625 Kotwicki, S., and Lauth, R.R. 2013. Detecting temporal trends and environmentally-driven changes in the  
626 spatial distribution of bottom fishes and crabs on the eastern Bering Sea shelf. *Deep-Sea Res. Pt.  
627 II* 94: 231-243. doi:10.1016/j.dsr2.2013.03.017.

628 Kruse, G.H. 2023. Are crabs in hot water? *Science* 382(6668): 260-261. doi:10.1126/science.adk7565.

629 Kruse, G.H., Daly, B.J., Fedewa, E.J., Stram, D.L., and Szuwalski, C.S. 2025. Ecosystem-based fisheries  
630 management of crab fisheries in the Bering Sea and Aleutian Islands. *Fish. Res.* 281: 107236.  
631 doi:10.1016/j.fishres.2024.107236.

632 Lambert, Y., and Dutil, J-D. 1997. Condition and energy reserves of Atlantic cod (*Gadus morhua*) during  
633 the collapse of the northern Gulf of St. Lawrence stock. *Can. J. Fish. Aquat. Sci.* 54(10): 2388-  
634 2400. doi:10.1139/f97-145.

635 Laufkötter, C., Zscheischler, J., and Frölicher, T.L. 2020. High-impact marine heatwaves attributable to  
636 human-induced global warming. *Science* 369(6511): 1621-1625.  
637 doi: .

638 Litzow, M.A., Fedewa, E.J., Malick, M.J., Connors, B.M., Eisner, L., Kimmel, D.G., Kristiansen, T.,  
639 Nielsen, J.M., and Ryznar, E.R. 2024. Human-induced borealization leads to the collapse of  
640 Bering Sea snow crab. *Nat. Clim. Change.* doi:10.1038/s41558-024-02093-0.

641 Lorentzen, G., Lian, F., and Siikavuopio, S.I. 2020. Live holding of snow crab (*Chionoecetes opilio*) at 1  
642 and 5 degrees C without feeding - Quality of processed clusters. *Food Control* 114: 9.  
643 doi:10.1016/j.foodcont.2020.107221.

644 Lovvorn, J.R., North, C.A., Kolts, J.M., Grebmeier, J.M., Cooper, L.W., and Cui, X.H. 2016. Projecting  
645 the effects of climate-driven changes in organic matter supply on benthic food webs in the  
646 northern Bering Sea. *Mar Ecol Prog Ser* 548: 11-30. doi:10.3354/meps11651.

647 Meier, S., Mjøs, S.A., Joensen, H., and Grahl-Nielsen, O. 2006. Validation of a one-step  
648 extraction/methylation method for determination of fatty acids and cholesterol in marine tissues.  
649 *J. Chromatogr. A* 1104(1-2): 291-298. doi:10.1016/j.chroma.2005.11.045

650 Mueter, F.J., and Litzow, M.A. 2008. Sea ice retreat alters the biogeography of the Bering Sea continental  
651 shelf. *Ecol. Appl.* 18(2): 309-320.

652 Mullowney, D., Baker, K., Szuwalski, C., Boudreaud, S., Cyrid, F., and Kaiserid, B. 2023. Sub-Arctic no  
653 more: Short-and long-term global-scale prospects for snow crab (*Chionoecetes opilio*) under  
654 global warming. *PLOS Clim.* 2(10): e0000294. doi:10.1371/journal.pclm.0000294.

655 Mullowney, D.R.J., and Rose, G.A. 2014. Is recovery of northern cod limited by poor feeding? The  
656 capelin hypothesis revisited. *ICES J. Mar. Sci.* 71(4): 784-793. doi:10.1093/icesjms/fst188.

657 Murphy, J.T., Hallowed, A.B., and Anderson, J.J. Snow crab spatial distributions: Examination of  
658 density-dependent and independent processes. In *Biology and Management of Exploited Crab  
659 Populations under Climate Change*. Anchorage, AK 2010. Edited by G.H. Kruse and G.L. Eckert  
660 and R.J. Foy and R.N. Lipcius and B. Sainte-Marie and D.L. Stram and D. Woodby. Alaska Sea  
661 Grant College Program, University of Alaska Fairbanks. pp. 49-79.

662 Murphy, J.T. 2020. Climate change, interspecific competition, and poleward vs. depth distribution shifts:  
663 Spatial analyses of the eastern Bering Sea snow and Tanner crab (*Chionoecetes opilio* and *C.  
664 bairdi*). *Fish. Res.* 223: 105417. doi: 10.1016/j.fishres.2019.105417.

665 Neubauer, P., Jensen, O.P., Hutchings, J.A., and Baum, J.K. 2013. Resilience and recovery of  
666 overexploited marine populations. *Science* 340(6130): 347-349. doi:10.1126/science.1230441.

667 Nielsen, J.M., Sigler, M.F., Eisner, L.B., Watson, J.T., Rogers, L.A., Bell, S.W., Pelland, N., Mordy,  
668 C.W., Cheng, W., Kivva, K., Osborne, S., and Stabeno, P. 2024. Spring phytoplankton bloom  
669 phenology during recent climate warming on the Bering Sea shelf. *Prog Oceanogr* 220: 103176.  
670 doi:<https://doi.org/10.1016/j.pocean.2023.103176>.

671 Notz, D., and Stroeve, J. 2016. Observed Arctic sea-ice loss directly follows anthropogenic CO<sub>2</sub>  
672 emission. *Science* 354(6313): 747-750. doi:10.1126/science.aag2345.

673 Ortiz, I., Wiese, F., Greig, A., 2013. Marine Regions Boundary Data for the Bering Sea Shelf and Slope,  
674 Version 1.0. UCAR/NCAR - Earth Observing Laboratory. <http://dx.doi.org/10.5065/D6DF6P6C>

675 Overland, J.E., and Stabeno, P.J. 2004. Is the climate of the Bering Sea warming and affecting the  
676 ecosystem? *EOS* 85(33): 309-316.

677 Overland, J.E., Siddon, E., Sheffield, G., Ballinger, T.J., and Szuwalski, C. 2024. Transformative  
678 ecological and human impacts from diminished sea ice in the northern Bering Sea. *Weather*  
679 *Clim. Soc.* 6(2): 303-313. doi:10.1175/WCAS-D-23-0029.1.

680 Overland, J.E., and Wang, M. 2025. Future climate change in the northern Bering Sea. *Int. J. Climatol.*  
681 45(1): e8697. doi:10.1002/joc.8697.

682 Parada, C., Armstrong, D.A., Ernst, B., Hinckley, S., and Orensanz, J. 2010. Spatial dynamics of snow  
683 crab (*Chionoecetes opilio*) in the eastern Bering Sea-putting together the pieces of the puzzle. *B*  
684 *Mar Sci* 86(2): 413-437.

685 R Core Team. 2023. R: A Language and Environment for Statistical Computing. R Foundation for  
686 Statistical Computing, Vienna, Austria. <<https://www.R-project.org/>>

687 Receveur, A., Bleil, M., Funk, S., Stöter, S., Gräwe, U., Naumann, M., Dutheil, C., and Krumme, U.  
688 2022. Western Baltic cod in distress: decline in energy reserves since 1977. *ICES J. Mar. Sci.*  
689 79(4): 1187-1201. doi:10.1093/icesjms/fsac042.

690 Regular, P.M., Buren, A.D., Dwyer, K.S., Cadigan, N.G., Gregory, R.S., Koen-Alonso, M., Rideout,  
691 R.M., Robertson, G.J., Robertson, M.D., Stenson, G.B., Wheeland, L.J., and Zhang, F. 2022.  
692 Indexing starvation mortality to assess its role in the population regulation of Northern cod.  
693 *Fisheries Research* 247: 106180. doi.org/10.1016/j.fishres.2021.106180.

694 Richar, J.I., and Foy, R.J. 2022. A novel morphometry-based method for assessing maturity in male  
695 Tanner crab, *Chionoecetes bairdi*. *Facets* 7: 1598-1616. doi:10.1139/facets-2021-0061.

696 Rohan S. 2024. akgfmaps: Alaska Groundfish and Ecosystem Survey Area Mapping. Available  
697 from <https://github.com/afsc-gap-products/akgfmaps> [accessed 29 January 2025].

698 Sherwood, G.D., Rideout, R.M., Fudge, S.B., and Rose, G.A. 2007. Influence of diet on growth,  
699 condition and reproductive capacity in Newfoundland and Labrador cod (*Gadus morhua*):  
700 Insights from stable carbon isotopes ( $\delta^{13}\text{C}$ ). *Deep-Sea Res. Pt. II Top. Stud. Oceanogr.* 54(23):  
701 2794-2809. doi:10.1016/j.dsr2.2007.08.007.

702 Shotwell, S.K., Blackhart, K., Cunningham, C., Fedewa, E., Hanselman, D., Aydin, K., Doyle, M., Fissel,  
703 B., Lynch, P., Ormseth, O., Spencer, P., and Zador, S. 2023. Introducing the ecosystem and  
704 socioeconomic profile, a proving ground for next generation stock assessments. *Coast.*  
705 *Manage.* 51(5-6): 319-352. doi:10.1080/08920753.2023.2291858.

706 Somerton, D.A., Weinberg, K.L., and Goodman, S.E. 2013. Catchability of snow crab (*Chionoecetes*  
707 *opilio*) by the eastern Bering Sea bottom trawl survey estimated using a catch comparison  
708 experiment. *Canadian Journal of Fisheries and Aquatic Sciences* 70(12): 1699-1708.  
709 doi:10.1139/cjfas-2013-0100.

710 Stabeno, P.J., and Bell, S.W. 2019. Extreme conditions in the Bering Sea (2017–2018): Record-breaking  
711 low sea-ice extent. *Geophys. Res. Letters* 46(15): 8952-8959. doi:10.1029/2019GL083816.

712 Stabeno, P.J., Farley, E.V., Kachel, N.B., Moore, S., Mordy, C.W., Napp, J.M., Overland, J.E., Pinchuk,  
713 A.I., and Sigler, M.F. 2012. A comparison of the physics of the northern and southern shelves of  
714 the eastern Bering Sea and some implications for the ecosystem. *Deep-Sea Res. Pt. II Top. Stud.*  
715 *Oceanogr.* 65-70: 14-30. doi:10.1016/j.dsr2.2012.02.019.

716 Stan Development Team. 2024. "RStan: the R interface to Stan." R package version 2.32.3, <https://mc-stan.org/>.

718 Stauffer, G. 2004. NOAA protocols for groundfish bottom trawl surveys of the Nation's fishery  
719 resources. U.S. Department of Commerce, NOAA, Technical Memorandum NMFS-SPO-65.

720 Stevenson, R.D., and Woods, W.A., Jr. 2006. Condition indices for conservation: new uses for evolving  
721 tools. *Integr. Comp. Biol.* 46(6): 1169-1190. doi:10.1093/icb/icl052.

722 Szwalski, C., Cheng, W., Foy, R., Hermann, A.J., Hollowed, A., Holsman, K., Lee, J., Stockhausen, W.,  
723 and Zheng, J. 2020. Climate change and the future productivity and distribution of crab in the  
724 Bering Sea. *ICES Journal of Marine Science*. doi:10.1093/icesjms/fsaa140.

725 Szwalski, C. 2022. Estimating time-variation in confounded processes in population dynamics  
726 modeling: A case study for snow crab in the eastern Bering Sea. *Fish. Res.* 251: 11.  
727 doi:10.1016/j.fishres.2022.106298.

728 Szwalski, C.S., Aydin, K., Fedewa, E.J., Garber-Yonts, B., and Litzow, M.A. 2023. The collapse of  
729 eastern Bering Sea snow crab. *Science* 382(6668): 306-310. doi:10.1126/science.adf6035.

730 Wang, M., and Overland, J. 2012. A sea ice free summer Arctic within 30 years: An update from CMIP5  
731 models. *Geophys. Res. Letters* 39: 18501. doi:10.1029/2012GL052868..

732

733

734

735

736

737

738

739

740

**Table 1.** Sample sizes for hepatopancreas collections from juvenile snow crab to estimate energetic condition in the collapsing eastern Bering Sea and non-collapsing northern Bering Sea portions of the snow crab population.

	2019	2021	2022	2023	2024	Total
Eastern Bering Sea	98	168	138	189	178	771
Northern Bering Sea	126	192	127	109		554
Total	224	360	265	298	178	1325

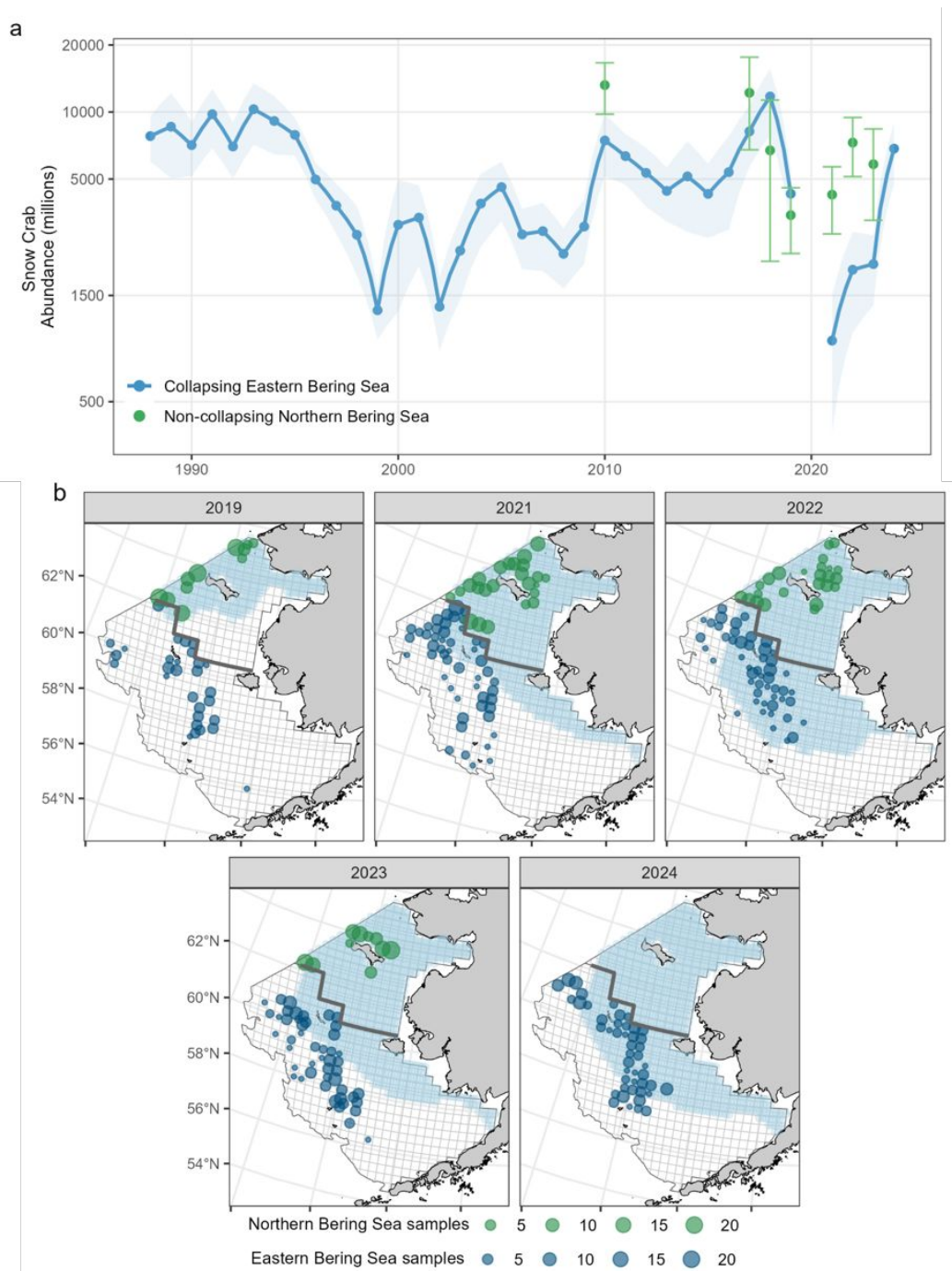


**Figure 1.** Study system. a) Abundance estimates for the collapsing eastern Bering Sea (blue line  $\pm$  95% CI) and non-collapsing northern Bering Sea (green points  $\pm$  95% CI) portions of the snow crab population. Note log scale on y-axis. b) Juvenile snow crab hepatopancreas sampling effort on eastern Bering Sea bottom trawl surveys (2019, 2021-2024) and northern Bering Sea bottom trawl surveys (2019, 2021-2023) relative to sea ice cover. Blue shaded areas indicate regions with mean March sea ice concentration  $\geq 15\%$ , grid cells indicate standard survey stations, heavy grey line indicates the boundary between the eastern and northern Bering Sea study regions, and green and blue bubbles indicate snow crab sample size by region. Note that the northern Bering Sea was not sampled in 2024. Maps use the Alaska Albers projection and NAD83 datum (Rohan 2024).

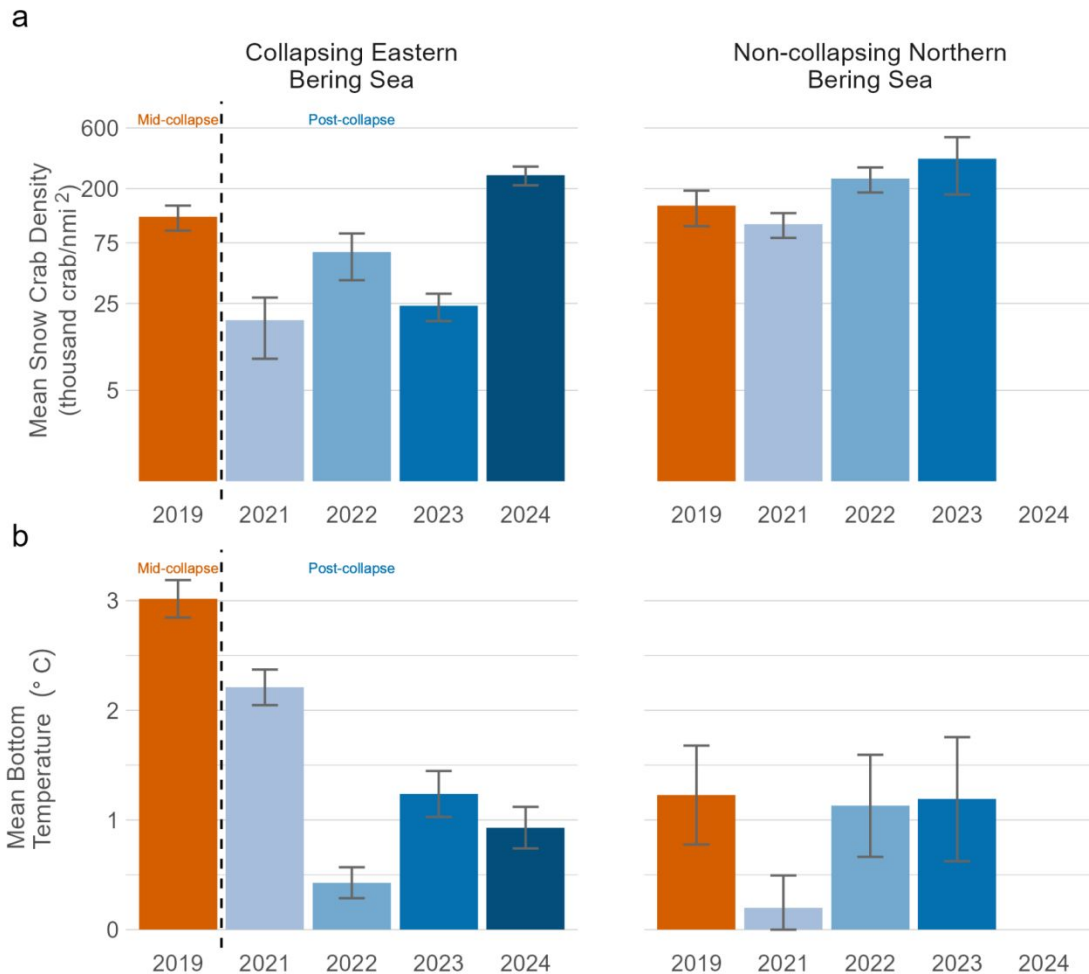


**Figure 2.** Observed snow crab densities and temperatures coinciding with the eastern Bering Sea population collapse and marine heatwave in 2019. a) Average snow crab population density ( $\pm$  SE) at sampled eastern and northern Bering Sea survey stations during (2019) and after (2021-2024) the eastern Bering Sea population collapse. Note log scale on y-axis. b) Average bottom temperature ( $\pm$  SE) at sampled eastern and northern Bering Sea survey stations. Note that the northern Bering Sea was not sampled in 2024.

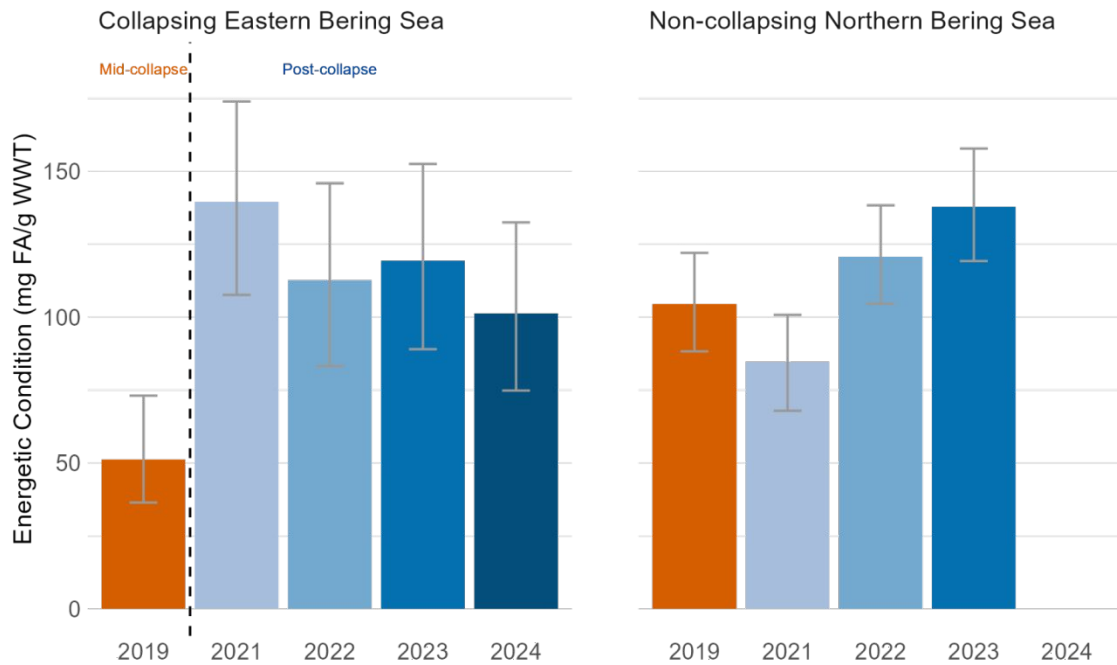


**Figure 3.** Annual estimates of Bering Sea snow crab energetic condition. Colors designate sampling years during the eastern Bering Sea population collapse (2019) and following the population collapse (2021-2024). Plotted values are posterior means of energetic condition (total fatty acids per wet weight) with 95% credible intervals from a Bayesian regression model controlling for crab size and seasonality.

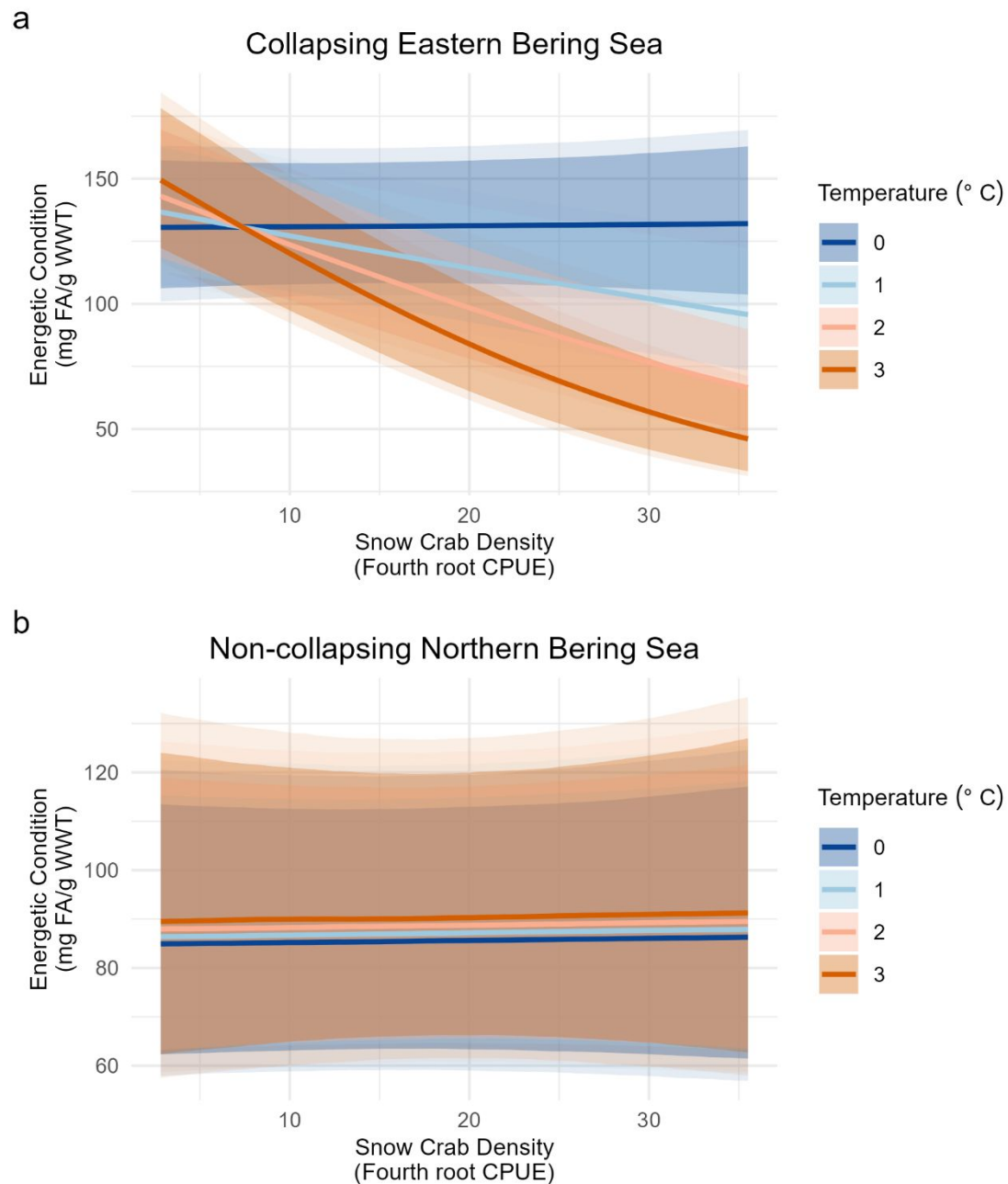


**Figure 4.** Population density and temperature effects on energetic condition of the collapsing eastern Bering Sea and non-collapsing northern Bering Sea portion of the snow crab population. (a) Predicted conditional effects (posterior means  $\pm$  90/95% CIs) of the interaction between snow crab density and bottom temperature on eastern Bering Sea snow crab energetic condition (total fatty acids per wet weight) across all years sampled (2019, 2021-2024); (b) and (c) Predicted conditional effects (posterior means  $\pm$  80/90/95% CIs) of the interaction between snow crab density and bottom temperature on northern Bering Sea snow crab energetic condition across all years sampled (2019, 2021-2023).

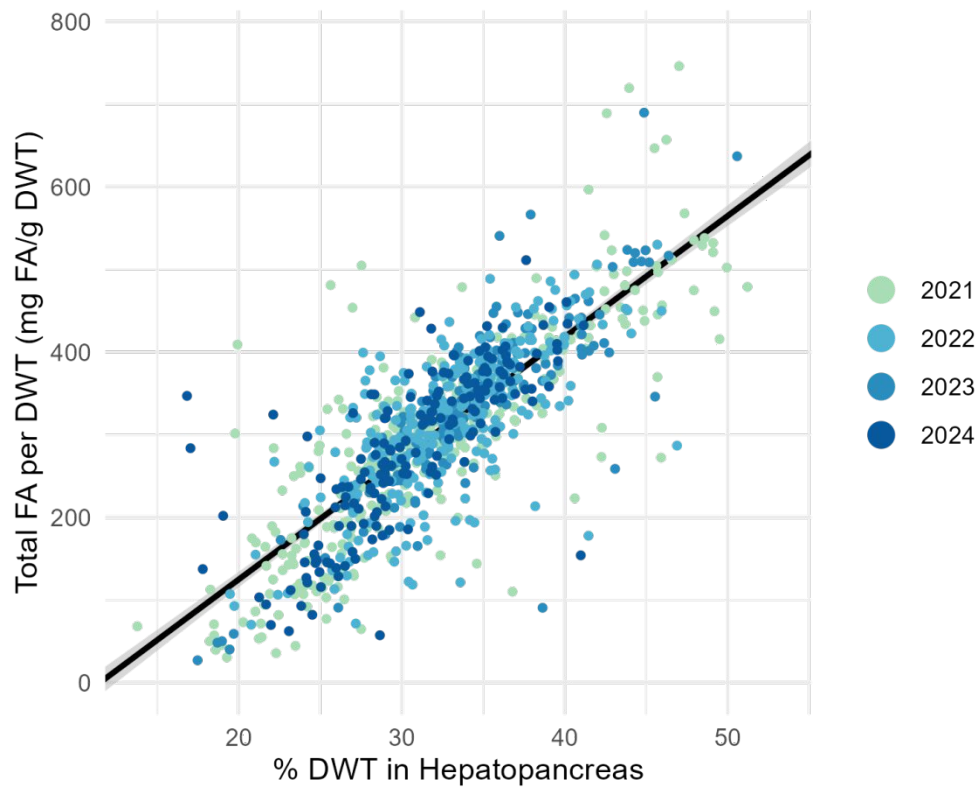


**Figure 5.** The linear relationship between the percentage dry weight and total fatty acids per dry weight of the hepatopancreas in juvenile snow crab. Plotted values are the predicted relationship and 95% credible intervals from a Bayesian regression model fit to observed data (2021-2024).